








## RESEARCH ARTICLE

WILEY

# Disruption of a *Plasmodium falciparum* patatin-like phospholipase delays male gametocyte exflagellation

Emma Pietsch <sup>1,2,3</sup> | Korbinian Niedermüller<sup>1,2,3</sup> | Mia Andrews <sup>4</sup> | Britta S. Meyer <sup>5</sup> | Tobias L. Lenz <sup>5</sup> | Danny W. Wilson <sup>4,6</sup> | Tim-Wolf Gilberger <sup>1,2,3</sup> | Paul-Christian Burda <sup>1,2,3</sup>

<sup>1</sup>Centre for Structural Systems Biology, Hamburg, Germany

<sup>2</sup>Bernhard Nocht Institute for Tropical Medicine, Hamburg, Germany

<sup>3</sup>University of Hamburg, Hamburg, Germany

<sup>4</sup>Research Centre for Infectious Diseases, School of Biological Sciences, University of Adelaide, Adelaide, South Australia, Australia

<sup>5</sup>Research Unit for Evolutionary Immunogenomics, Department of Biology, University of Hamburg, Hamburg, Germany

<sup>6</sup>Burnet Institute, Melbourne, Victoria, Australia

## Correspondence

Tim-Wolf Gilberger and Paul-Christian Burda, Centre for Structural Systems Biology, Hamburg, Germany.  
Email: [gilberger@bnitm.de](mailto:gilberger@bnitm.de) and [burda@bnitm.de](mailto:burda@bnitm.de)

## Funding information

Alexander von Humboldt-Stiftung; Australian Research Council; DAAD/Universities Australia; Deutsche Forschungsgemeinschaft, Grant/Award Number: 414222880 and 446556156; DFG within the SPP2225

## Abstract

An essential process in transmission of the malaria parasite to the *Anopheles* vector is the conversion of mature gametocytes into gametes within the mosquito gut, where they egress from the red blood cell (RBC). During egress, male gametocytes undergo exflagellation, leading to the formation of eight haploid motile microgametes, while female gametes retain their spherical shape. Gametocyte egress depends on sequential disruption of the parasitophorous vacuole membrane and the host cell membrane. In other life cycle stages of the malaria parasite, phospholipases have been implicated in membrane disruption processes during egress, however their importance for gametocyte egress is relatively unknown. Here, we performed comprehensive functional analyses of six putative phospholipases for their role during development and egress of *Plasmodium falciparum* gametocytes. We localize two of them, the prodrug activation and resistance esterase (PF3D7\_0709700) and the lysophospholipase 1 (PF3D7\_1476700), to the parasite plasma membrane. Subsequently, we show that disruption of most of the studied phospholipase genes does neither affect gametocyte development nor egress. The exception is the putative patatin-like phospholipase 3 (PF3D7\_0924000), whose gene deletion leads to a delay in male gametocyte exflagellation, indicating an important, albeit not essential, role of this enzyme in male gametogenesis.

## KEYWORDS

egress, exflagellation, gametocyte, malaria, phospholipase

## 1 | INTRODUCTION

Egress from red blood cells (RBCs) represents an essential process for the transmission of the human malaria parasite *Plasmodium falciparum* to its mosquito vector. It is induced by ingestion of mature sexual parasite stages called gametocytes by female *Anopheles*

mosquitoes during a blood meal. Within minutes after ingestion, gametocytes become activated in the mosquito midgut by a drop in temperature, a rise in pH, and the presence of the mosquito-derived molecule xanthurenic acid (Bennink et al., 2016). Following their activation, they undergo gametogenesis, whereby each female gametocyte produces a single immotile macrogamete,

This is an open access article under the terms of the [Creative Commons Attribution](https://creativecommons.org/licenses/by/4.0/) License, which permits use, distribution and reproduction in any medium, provided the original work is properly cited.

© 2023 The Authors. *Molecular Microbiology* published by John Wiley & Sons Ltd.

whereas a male gametocyte produces eight flagella-like microgametes in a process called exflagellation. After their release from host RBCs, macrogametes and microgametes fuse to form the zygote, which later develops into the motile ookinete (Kuehn & Pradel, 2010).

During their intracellular maturation, gametocytes are surrounded by a parasitophorous vacuole membrane (PVM), which needs to be ruptured before and in addition to the RBC membrane for efficient release of gametes. Membrane rupture is facilitated by the exocytosis of specialized secretory vesicles of the parasites. These include the osmiophilic bodies that release a variety of egress-related proteins into the parasitophorous vacuole lumen (Flieger et al., 2018). In addition, other vesicles are released during egress that contain the perforin-like protein PPLP2, which is necessary for erythrocyte lysis (Deligianni et al., 2013; Wirth et al., 2014).

In other life cycle stages of malaria parasites, membrane rupture has been shown to be partially mediated by a secreted phospholipase with a lecithin:cholesterol acyltransferase-like domain. Rodent malaria *Plasmodium berghei* parasites missing this enzyme were defective in liver stage egress due to impaired PVM rupture (Burda et al., 2015) and conditional knockout of the same enzyme in *P. falciparum* negatively affected parasite release of asexual blood stage parasites from RBCs (Ramaprasad et al., 2023). The importance of phospholipases for membrane disruption processes during gametocyte egress is relatively unknown. Until now, only the patatin-like phospholipase 1 (PNPLA1) PF3D7\_0209100 has a known potential function in this regard. Its conditional knockout reduced efficiency of gametocyte egress possibly by interfering with the release of egress-associated vesicles (Singh et al., 2019).

In this study, we performed a comprehensive functional analysis of six putative phospholipases for their role during development and egress of *P. falciparum* gametocytes. We show that five of the six phospholipases are likely dispensable for these processes but reveal that parasites lacking the putative PNPLA PF3D7\_0924000 show a significant delay in efficient exflagellation of male gametocytes, suggesting an important but not essential function of this enzyme in male gametogenesis.

## 2 | RESULTS

### 2.1 | *P. falciparum* expresses at least 15 putative phospholipases during gametocyte development

The genome of *P. falciparum* includes 26 genes that encode for proteins containing putative lipase/phospholipase-related domains (Burda et al., 2023). For 15 of these, there exists mass spectrometric evidence for expression in gametocytes (Florens et al., 2002; Lasonder et al., 2016; Silvestrini et al., 2010) (Figure S1), indicating a potential function in this parasite stage. Six of these gametocyte-expressed enzymes have a predicted signal peptide or contain transmembrane domains, suggesting they might be targeted into

the secretory pathway and could be involved in membrane modification and/or disruption during the egress process (Figure S1). Given our previous results that disruption of the PF3D7\_0908000 homolog in *P. berghei* did not result in a phenotype throughout the parasite life cycle (Burda et al., 2017) and the fact that the putative PNPLA2 (PF3D7\_1358000) is important for mitochondrial function (Pietsch et al., 2023), we focused on the remaining four proteins (PF3D7\_0731800, PF3D7\_0924000, PF3D7\_1411900, PF3D7\_1412000) containing a predicted signal peptide or transmembrane domains for functional characterization in gametocytes. Additionally, we included the putative phospholipases PF3D7\_1476700 and PF3D7\_0709700 into our assays, as both show peak expression in stage V gametocytes based on RNAseq analysis (López-Barragán et al., 2011) (Figure S1).

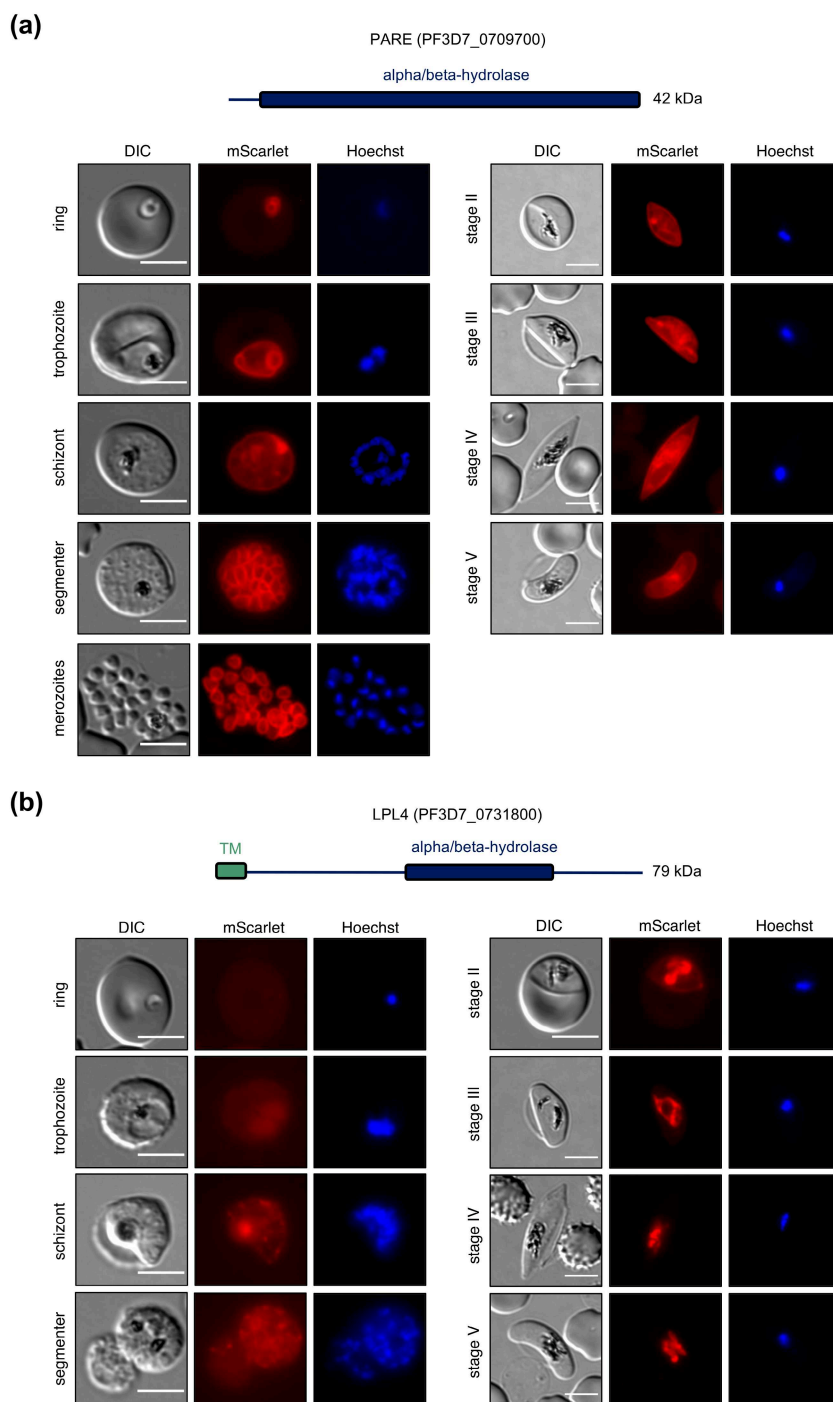
To investigate the functional conservation of the six candidate genes among apicomplexan parasites, we employed a reciprocal BLAST search strategy to investigate the presence or absence of orthologous proteins within a number of species encompassing relevant alveolates. This provided insights into the conservation and divergence of the different proteins in *P. falciparum* compared to other species, such as the potential existence of ortholog relationships (Figure S2, Table S1).

### 2.2 | The six selected putative phospholipases show various localization patterns in blood stage parasites

To study protein localization of the six selected putative phospholipases, we performed endogenous C-terminal tagging with mScarlet or mNeonGreen and analyzed transgenic parasites lines using live-cell microscopy. For genetic modification of the respective gene loci, we used the selection-linked integration (SLI) system (Birnbaum et al., 2017) in NF54/iGP2 parasites (Boltryk et al., 2021). This parasite line enables the production of high numbers of synchronous gametocytes and is transmission-competent, which means that it has maintained its ability to form gametes. Gametocyte commitment in this line is induced by conditional overexpression of the sexual commitment factor GDV1 (Boltryk et al., 2021). Correct integration of the respective constructs was verified by PCR (Figure S3) and expression of the respective correctly sized mScarlet/mNeonGreen fusion proteins was further confirmed by western blot analysis (Figure S4).

The prodrug activation and resistance esterase (PARE, PF3D7\_0709700) showed a peripheral localization throughout asexual and sexual blood stage development which was also clearly visible in free merozoites suggesting that PARE mostly localizes to the parasite plasma membrane (PPM) (Figure 1a). However, in gametocytes PARE was additionally visible in intracellular vesicular structures. The lysophospholipase 4 (LPL4, PF3D7\_0731800) (Asad et al., 2021) was not visible in ring and trophozoite stage parasites, while schizont stages displayed a weak punctuate pattern of LPL4-mScarlet in the cytoplasm and some signal in the food

**FIGURE 1** Localization analysis of PARE and LPL4. Parasites expressing endogenously tagged PARE-mScarlet (a) and LPL4-mScarlet (b) were analyzed during asexual and sexual blood stage development by live-cell microscopy. Nuclei were stained with Hoechst. Scale bars = 5  $\mu$ m. DIC, differential interference contrast. Schematic representations of the functional domains of the two proteins are shown on top of the images. TM, transmembrane domain.



vacuole that was likely derived from unspecific hemozoin autofluorescence. During gametocyte development, LPL4-mScarlet localized mainly to the food vacuole. In addition, a peripheral signal was visible in some gametocytes (Figure 1b). To validate the specificity of the observed signals, we imaged NF54/iGP2 parental wild type (WT) asexual blood stage parasites as well as gametocytes with the same imaging settings used for analysis of transgenic parasite lines expressing mScarlet fusion proteins at low or undetectable levels (Figure S5). This excluded that the observed food vacuole signal in LPL4-mScarlet gametocytes was derived from unspecific background fluorescence.

The putative PNPLA PF3D7\_0924000, from here on referred to as PNPLA3, since PNPLA1 and PNPLA2 have already been described (Flammersfeld et al., 2020; Pietsch et al., 2023; Singh et al., 2019), could not be detected in asexual stages except for some autofluorescence of the hemozoin within the food vacuole as concluded from imaging WT parasites with the same settings. In gametocytes, a vesicular and diffuse cytoplasmic signal of PNPLA3-mScarlet was observed, which was clearly higher than in parental WT gametocytes (Figures 2a and S5). The putative phospholipase PF3D7\_1411900, here termed phospholipase 39 (PL39) due to its predicted molecular weight of 39 kDa, showed a possibly

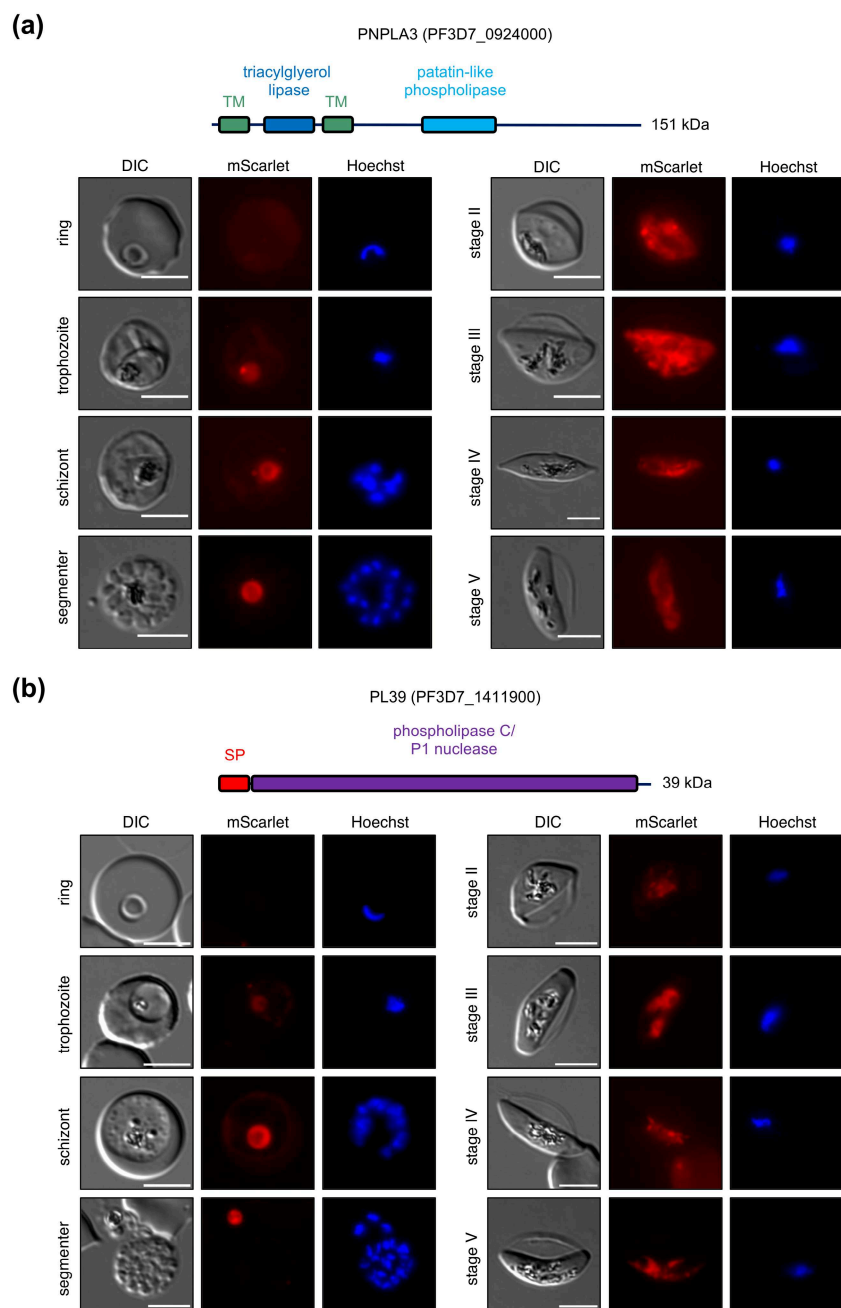


**FIGURE 2** Localization analysis of PNPLA3 and PL39. Parasites expressing endogenously tagged PNPLA3-mScarlet (a) and PL39-mScarlet (b) were analyzed during asexual and sexual blood stage development by live-cell microscopy. Nuclei were stained with Hoechst. Scale bars = 5  $\mu$ m. DIC, differential interference contrast. Schematic representations of the functional domains of the two proteins are shown on top of the images. SP, signal peptide; TM, transmembrane domain.

unspecific signal in the food vacuole in all asexual and sexual blood stage parasites (Figure 2b).

Interestingly, another putative phospholipase (PF3D7\_1412000) is expressed from the neighboring gene locus. It has a predicted molecular weight of 38 kDa and is hence referred to as phospholipase 38 (PL38). In contrast to PL39, PL38-mScarlet displayed a punctuate localization pattern in schizonts and free merozoites, possibly suggesting a localization to the apical organelles of the parasite. In all other intraerythrocytic asexual stages and gametocytes no signal or only autofluorescence of the hemozoin could be observed, supporting a potential schizont-specific function of PL38 (Figure 3a). Confocal airyscan microscopy-based colocalization analysis of PL38 with the microneme marker AMA1 and the rhoptry marker RAP1 did not reveal an exclusive

localization to any of the two but did confirm apical localization of the protein (Figure S6). The lysophospholipase 1 (LPL1, PF3D7\_1476700) (Asad et al., 2021) fused to mScarlet showed a peripheral localization in gametocytes, while no signal was visible in asexual blood stages of this parasite line (Figure S7). Given that evidence for expression of LPL1 in asexual blood stages was provided previously (Asad et al., 2021), we generated an additional parasite line, in which the gene was C-terminally tagged with the much brighter green fluorescent protein mNeonGreen (Shaner et al., 2013). This genetic modification was performed in a 3D7 cell line that fully supports gametocyte development (Filarsky et al., 2018). Successful integration of the targeting construct was confirmed by PCR (Figure S3) and correct expression of the mNeonGreen fusion protein was verified by western blot analysis

**FIGURE 3** Localization analysis of PL38 and LPL1. Parasites expressing endogenously tagged PL38-mScarlet (a) and LPL1-mNeonGreen (b) were analyzed during asexual and sexual blood stage development by live-cell microscopy. Nuclei were stained with Hoechst. Scale bars = 5  $\mu$ m. DIC, differential interference contrast. Schematic representations of the functional domains of the two proteins are shown on top of the images. SP, signal peptide.

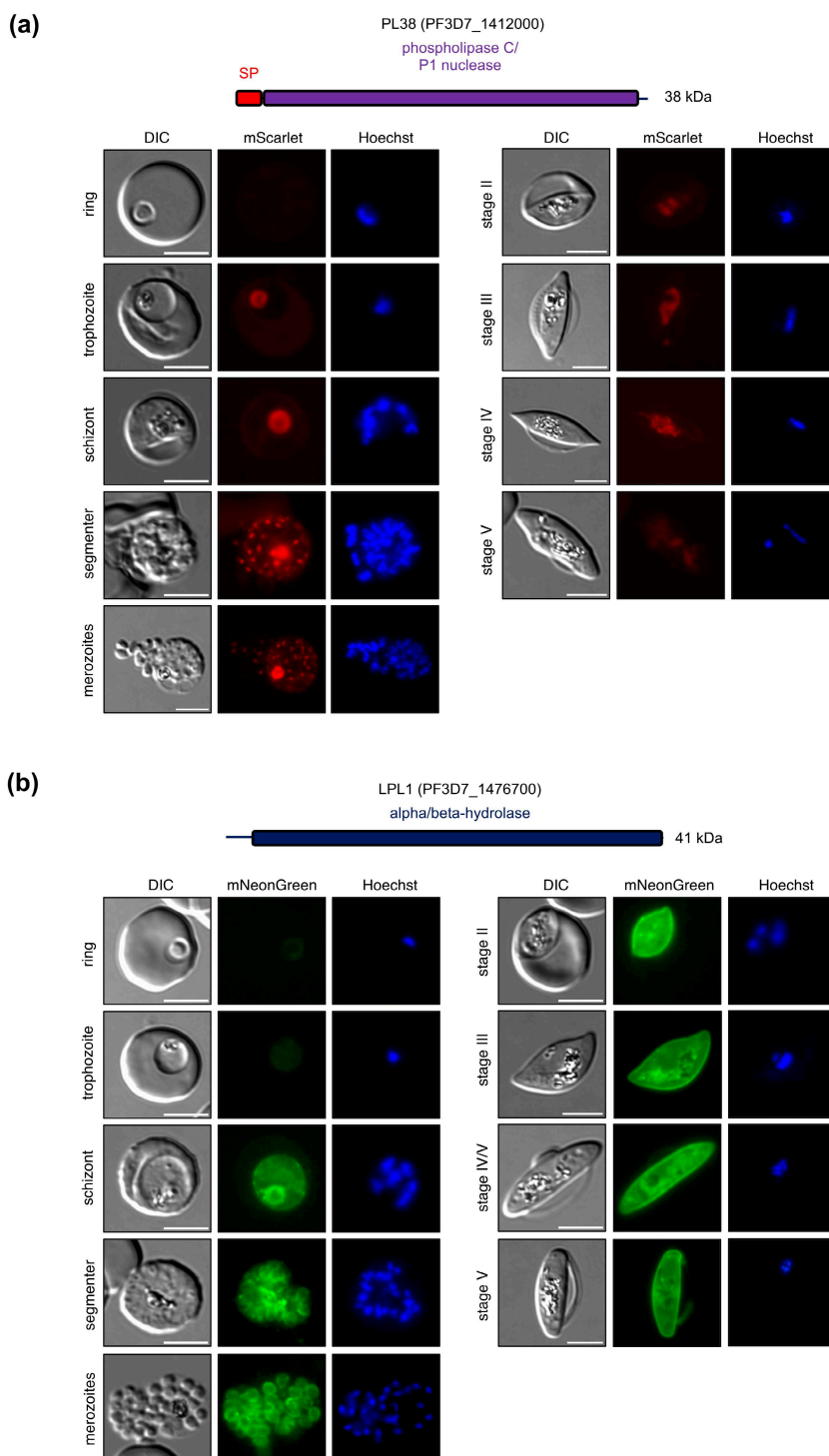


(Figure S4). LPL1-mNeonGreen displayed a strong peripheral signal throughout gametocyte development in line with the results of the LPL1-mScarlet line. In contrast to LPL1-mScarlet, however, a weaker peripheral signal was also observed for LPL1-mNeonGreen in schizonts as well as free merozoites (Figure 3b). Taken together, this suggests that LPL1 localizes to the PPM in both asexual stages and gametocytes and that its apparently lower expression levels in asexual blood stages presumably prevented its detection in the LPL1-mScarlet parasite line.

## 2.3 | Loss of individual phospholipases does not impair gametocyte development

To probe into the physiological function of the six putative phospholipases for gametocyte development and egress, we next performed targeted gene disruption (TGD) using the SLI system (Birnbaum et al., 2017) in the NF54/iGP2 background (Boltryk et al., 2021) and deleted 48%–82% of their coding sequence (Figure S8a,b). Correct integration of the respective targeting constructs was confirmed by



PCR (Figure S8c). Previously, we showed that five of the six phospholipases (PARE, LPL4, PNPLA3, PL39, and PL38) are non-essential for asexual blood stage development using the same targeting constructs (Burda et al., 2023). We thus only analyzed asexual blood stage proliferation of LPL1-TGD parasites. This, however, did not reveal an impaired growth in the presence or absence of 2 mM choline as compared to WT parasites, suggesting that LPL1 plays a non-essential or redundant function in asexual blood stage development (Figure S9).

To investigate the function of the selected phospholipases for gametocyte development, we induced gametocyte commitment as previously described (Boltryk et al., 2021) and followed gametocyte development over 2 weeks. Gametocyte survival rates, calculated by the ratio of gametocytemia on day 11 and day 5 of gametocyte development, were not significantly different between WT and TGD parasite lines (Figure S10). In line with this, quantification of gametocyte stages over the 11-day course of gametocytogenesis of all phospholipase-TGD lines revealed no major defect in gametocyte maturation (Figure 4). Taken together, these data suggest that the six analyzed putative phospholipases are dispensable for gametocyte development.

## 2.4 | Disruption of PNPLA3 delays male gametocyte exflagellation

Next, we analyzed gamete egress from mature stage V gametocytes. During this process, male gametocytes undergo a striking transformation resulting in the formation of eight haploid motile microgametes, while female gametes maintain their spherical shape after egress from the RBC (Kuehn & Pradel, 2010). To study whether gametocyte egress is affected in the TGD parasite lines, we used an established egress assay based on live-cell fluorescence microscopy (Figure 5a,b) (Suárez-Cortés et al., 2014). For this, the RBC membrane of RBCs infected with mature stage V gametocytes was stained using the live-cell dye iFluor555-wheat germ agglutinin (WGA) before activation. Subsequently, gametocytes were activated for 20 min and parasite morphology (falciform shape versus spherical shape) as well as the WGA staining pattern (WGA-positive versus WGA-negative) were investigated (Suárez-Cortés et al., 2014). As expected, the vast majority of non-activated gametocytes showed a falciform shape with strong WGA staining of the erythrocyte membrane, while after activation most gametocytes displayed a round morphology and were WGA-negative, indicating successful egress from the host RBC (Figure 5c-h). Hereby, no major differences between WT and TGD parasite lines were observed, indicating that all of the six tested phospholipases are dispensable for gamete egress. To further analyze egress, we also separately quantified exflagellation rates of male gametocytes on four subsequent days from day 11 until day 14 of gametocyte development. To that end, we activated gametocytes for 12 min and subsequently determined the percentage of exflagellating gametocytes within the next 5 min. PARE-TGD and LPL1-TGD gametocytes showed similar exflagellation rates to WT parasites,

while LPL4-TGD, PL39-TGD, and PL38-TGD showed significantly higher exflagellation rates compared to WT parasites (Figures 6 and S11). In line with the WGA staining-based egress assay, we can thus conclude that none of these five putative phospholipases plays an essential role in gametocyte exflagellation. Remarkably, PNPLA3-TGD gametocytes showed a significant reduction in exflagellation within the initial 5 min of observation time. Extending observation time by 10 min resulted in exflagellation rates similar to WT parasites (Figures 6c and S11), suggesting that loss of PNPLA3 delays efficient exflagellation but does not fully disrupt this process.

## 3 | DISCUSSION

Phospholipases were shown to have important functions for asexual intraerythrocytic development and egress of malaria blood and liver stage parasites (Burda et al., 2015, 2023; Pietsch et al., 2023; Ramaprasad et al., 2023). We here aimed to expand the functional characterization of these enzymes and investigated the role of six putative phospholipases for gametocytogenesis and gametocyte egress.

Two putative phospholipases analyzed in this study were PARE and LPL1. PARE was previously reported to have esterase activity and to activate esterified pepstatin, a peptidyl inhibitor of malarial aspartyl proteases, although its localization in the parasite had not yet been determined (Istvan et al., 2017). By endogenous tagging, we now localized PARE and LPL1 to the PPM in asexual and sexual blood stages of the parasite. In addition to this, we showed that disruption of PARE and LPL1 does not affect asexual blood stage development (this study and (Burda et al., 2023)), arguing for a redundant function of both enzymes under in vitro conditions. These localization and functional data regarding LPL1 differ to a previous study that localized LPL1 to a multi-vesicular neutral lipid-rich body next to the food vacuole in asexual blood stages and that proposed an essential role of LPL1 in neutral lipid synthesis contributing to hemozoin formation in the parasite (Asad et al., 2021). While the reasons for the observed differences in LPL1 localization remain unclear, the absence of a growth defect in asexual blood stages due to LPL1 disruption could be related to the different methods used for the inactivation of LPL1. While (Asad et al., 2021) employed a conditional degradation approach for ablating LPL1 expression, we used targeted gene disruption in this study involving selection of transgenic parasites over several intraerythrocytic cycles that may possibly enable parasites to adapt to the loss of LPL1 through a currently unknown mechanism.

Two other putative phospholipases that we analyzed in this study were PL39 and PL38, which both contain predicted signal peptides and phospholipase C/P1 nuclease domains. Enzymes containing these domains are typically involved in phosphate ester hydrolysis of lipids or nucleic acids (Coleman, 1992; Desai & Shankar, 2003). The genomic proximity of *pl39* and *pl38* and the existence of only one single orthologue in the rodent malaria parasite *P. berghei* at this genomic location (according to PlasmoDB.org,

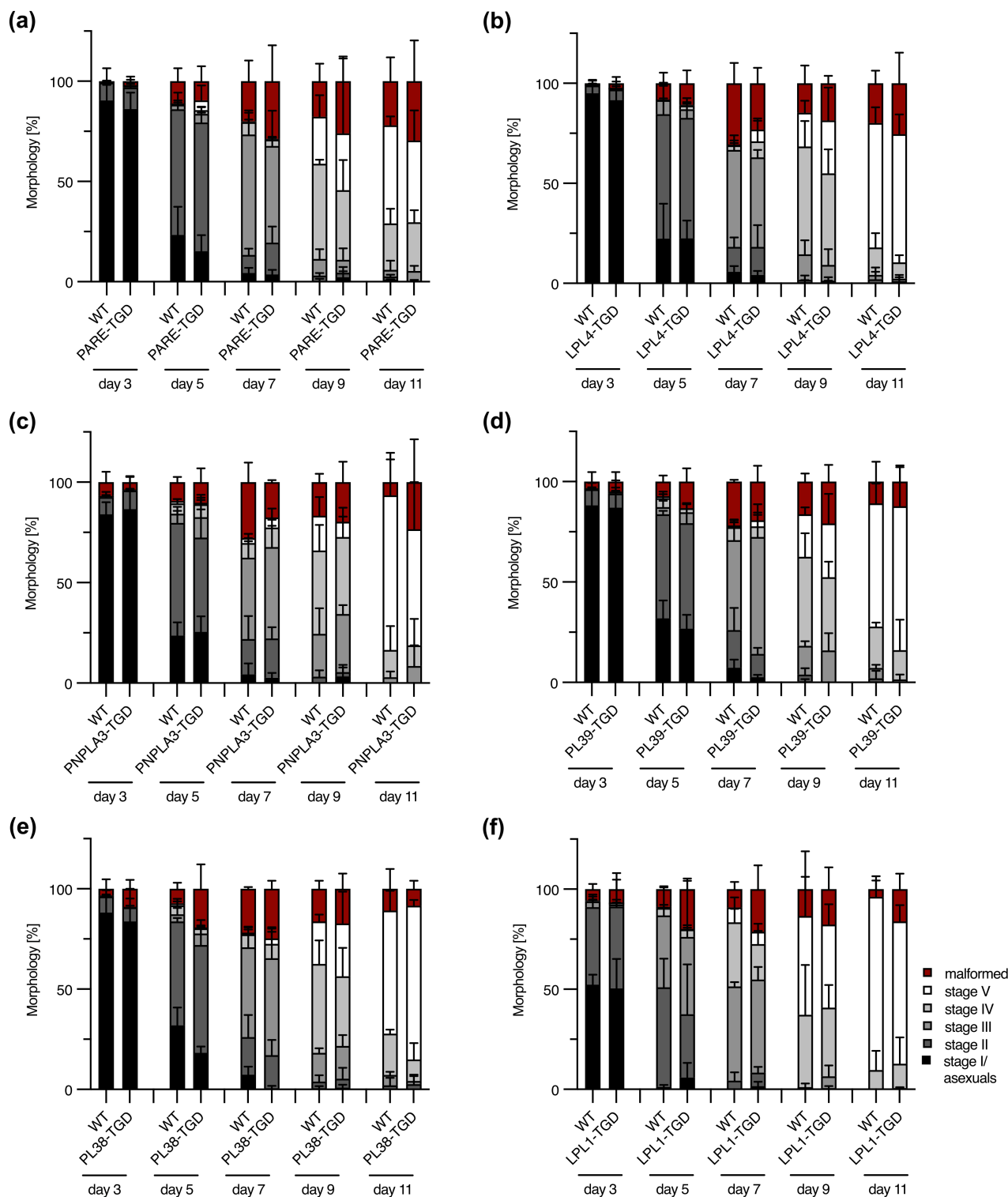


**FIGURE 4** Disruption of the six individual genes encoding for putative phospholipases does not affect gametocyte maturation. (a–f) Quantification of gametocyte stages on the days of gametocyte development indicated below the graphs by counting Giemsa-stained thin blood smears. Shown are means + SD of three independent experiments, in which the following total numbers of gametocytes were counted: Day 3: 292–479, Day 5: 175–376, Day 7: 94–258, Day 9: 76–211, Day 11: 37–206. In some experiments, NF54/iGP2 WT gametocytes served as a control for several TGD lines in parallel. (a) PARE-TGD, (b) LPL4-TGD, (c) PNPLA3-TGD, (d) PL39-TGD, (e) PL38-TGD, and (f) LPL1-TGD.

(Aurrecoechea et al., 2009)) indicates that these loci might have arisen from gene duplication. However, as PL39 and PL38 display only 46% sequence identity (according to ClustalW), they

may have diverged to serve distinct functions over the course of evolution. In line with this, PL38 displayed a possible apical localization in late schizonts, while no such localization was observed

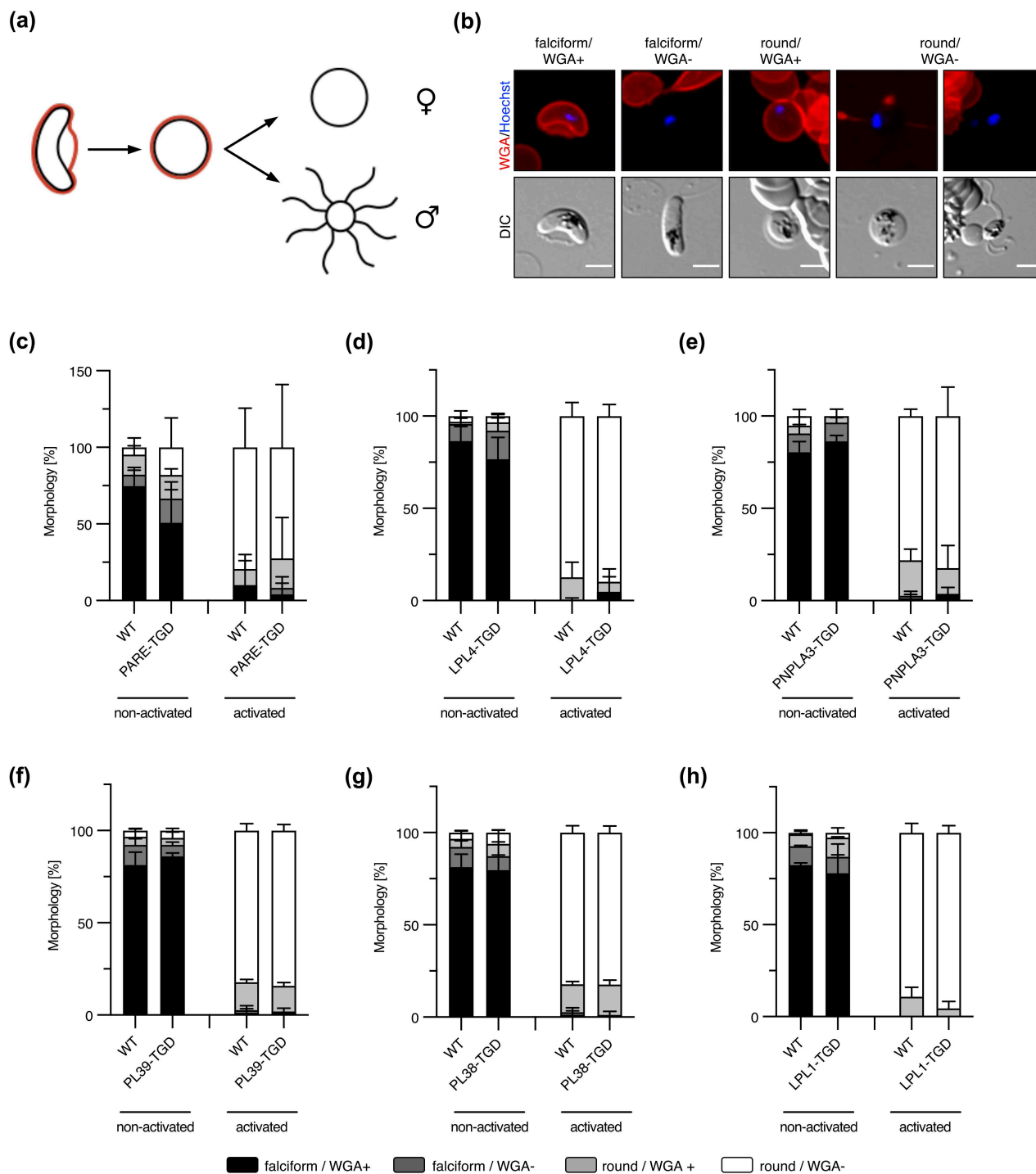


**FIGURE 5** None of the putative phospholipase-TGD lines displays a defect in gamete egress. (a) Schematic of the gamete egress assay. On day 14 of gametocytogenesis, the RBC membrane was stained with iFluor555-WGA (red). Upon activation, gametocytes first round up before egressing from the RBC thereby losing the iFluor555-WGA signal. Female gametocytes retain a round shape, while male gametocytes form eight motile flagella. (b) Representative images of the four categories used to classify gametocytes/gametes in the gamete egress assay. Staining with iFluor555-WGA (red) and Hoechst (blue). DIC, differential interference contrast. Scale bars = 5 μm. Please note that the very right image displays a male gametocyte in the process of exflagellation. Exflagellation was visible in 2.3% of the analyzed WT parasites (435 gametocytes analyzed, derived from 11 independent experiments). (c–h) Imaging-based gamete egress assays with (c) PARE-TGD, (d) LPL4-TGD, (e) PNPLA3-TGD, (f) PL39-TGD, (g) PL38-TGD, and (h) LPL1-TGD gametocytes. Gametocytes were imaged non-activated and after activation for 20 min. At least 20 parasites were imaged per condition in each independent experiment. Shown are means + SD of three independent experiments.



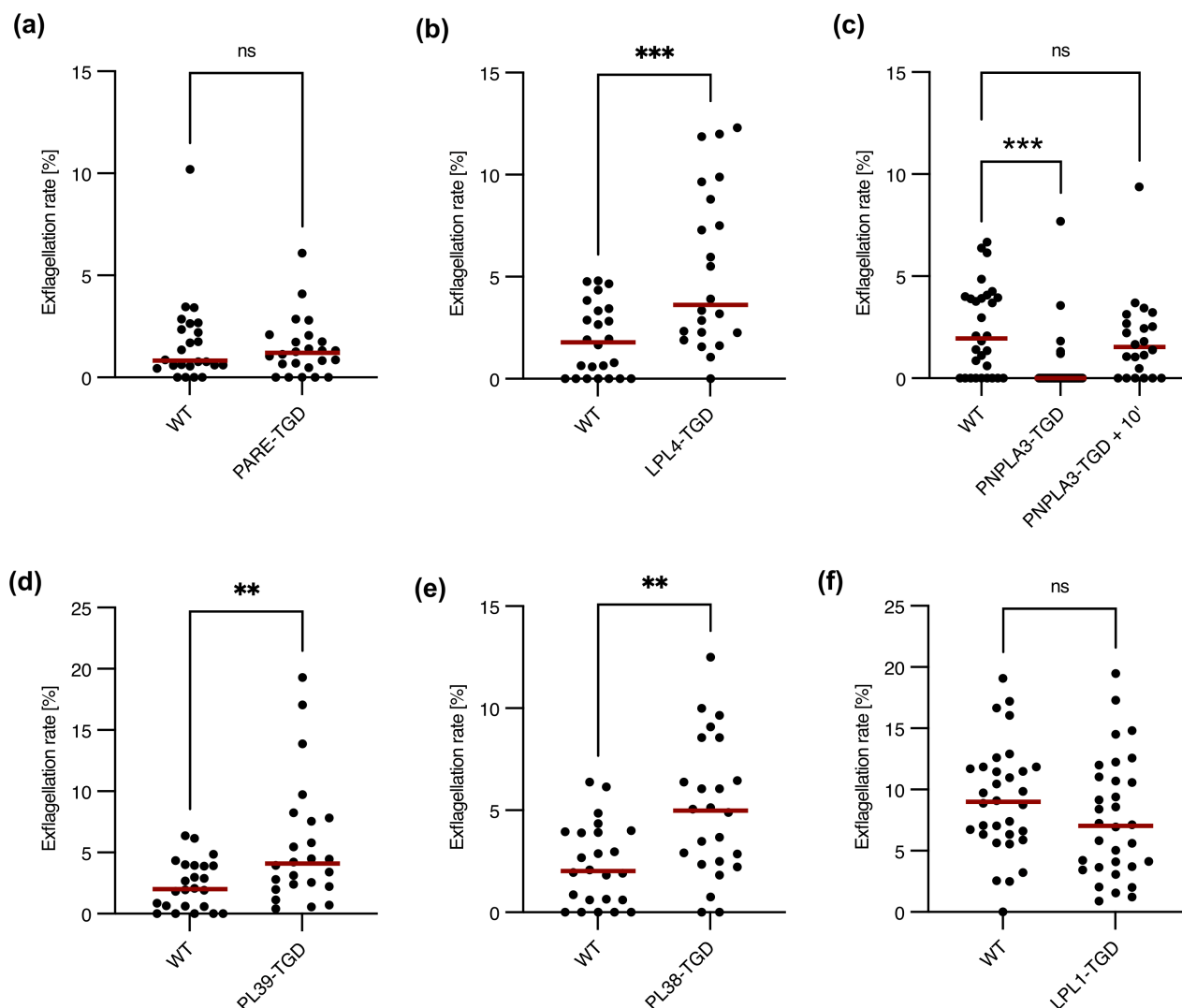


**FIGURE 6** PNPLA3-TGD parasites show a delay in male gametocyte exflagellation. (a–f) Exflagellation assays of (a) PARE-TGD, (b) LPL4-TGD, (c) PNPLA3-TGD (includes data with 10 additional minutes of exflagellation time), (d) PL39-TGD, (e) PL38-TGD, and (f) LPL1-TGD gametocytes. Graphs display superplots of at least three independent experiments. For each of the independent experiments, exflagellation was checked in technical duplicates on four subsequent days (day 11–day 14 of gametocyte development). Red lines indicate the median of all exflagellation rates observed across all days and independent experiments for the respective parasite line. For statistical analysis of the results, an unpaired students t-test was used (\*\* $p < 0.01$ ; \*\*\* $p < 0.0005$ ; n.s., not significant). In some experiments, NF54/iGP2 gametocytes served as control for several TGD lines in parallel. Exflagellation rates of the different parasite lines on the individual days are displayed in [Figure S11](#).

for PL39. Interestingly, the *Toxoplasma gondii* patatin-like phospholipase TgPL3 (TGME49\_305140) has been localized to the apical pole where its phospholipase activity is necessary for rhoptry secretion (Wilson et al., 2020). We speculate that the putative phospholipase activity of PL38 might similarly contribute to invasion. However, gene deletion did not affect asexual blood stage proliferation, suggesting an unimpaired invasion process of PL38-deficient parasites (Burda et al., 2023).

To explore the role of the six selected putative phospholipase candidates for gametocytogenesis and gametocyte egress, we performed targeted gene disruption of the individual genes. We then analyzed sexual blood stage development of the resulting mutant parasite lines. This revealed that gametocyte survival and maturation were not affected by the individual disruption of the six selected

putative phospholipases, suggesting that, similar to our results obtained in asexual blood stages (Burda et al., 2023), a high level of functional redundancy also exists among the parasite phospholipases during sexual blood stage development.

A live-cell fluorescence microscopy-based egress assay using the RBC membrane stain WGA (Suarez-Cortés et al., 2014) did not reveal any substantial differences in gametocyte egress between WT and mutant parasite lines. Interestingly, however, separately quantifying exflagellation rates of male gametocytes revealed that parasites lacking the PNPLA3 showed a significant delay in efficient exflagellation of male gametocytes indicating a critical, yet not essential, role of this enzyme in male gametogenesis. It is important to note that exflagellation rates of PNPLA3-TGD parasites reached WT levels, when the analysis time was extended for 10 min. Since

activation of gametocytes for the WGA assay was done for 20 min, while 12 min of gametocyte activation were used for the exflagellation assay, the extended time for gametocyte activation could explain why the PNPLA3-associated phenotype in exflagellation was not observed in the WGA-based egress assay. What specific role PNPLA3 might play in the exflagellation process remains to be elucidated. Endogenous tagging of PNPLA3 with mScarlet revealed a vesicular and diffuse cytoplasmic localization pattern of the protein in gametocytes arguing against a direct function of PNPLA3 in disruption of the PVM or the host cell membrane. In asexual PNPLA3-mScarlet blood stage parasites, only hemozoinderived autofluorescence could be observed, suggesting absence of expression in this parasite stage. This differs to a recent study, in which a PNPLA3-specific antiserum was used in immunofluorescence analysis (Shunmugam et al., 2023). Here, a diffuse cytoplasmic and punctated localization pattern for PNPLA3 in asexual blood stages was seen, indicating that PNPLA3 might also be expressed to a certain level at this time of parasite development.

A diffuse cytoplasmic localization during asexual and sexual blood stage development was also observed by two independent studies for another PNPLA of the parasite, referred to as PNPLA1 (PF3D7\_0209100) (Flammersfeld et al., 2020; Singh et al., 2019). Both studies, however, differed in their conclusions regarding the functional role of this enzyme. Flammersfeld et al. provided evidence for a role of PNPLA1 in gametocyte induction (Flammersfeld et al., 2020) while in the study of Singh et al. conditional inactivation of PNPLA1 reduced efficiency of gametocyte egress possibly by interfering with the release of egress-associated vesicles (Singh et al., 2019). The latter findings are of particular interest for the present study, as a similar function linked to the release of egress-associated vesicles might also be performed by PNPLA3. Given that conditional inactivation of PNPLA1 only resulted in a partial egress phenotype, both enzymes might even work together during egress, a scenario that should be explored in future studies by generating mutants that lack both enzymes.

Taken together, our data suggest that all six phospholipase candidates may have redundant functions for gametocyte development and gamete egress. However, PNPLA3 might have a role in efficient exflagellation of male gametocytes, identifying it as a novel player in this important process for transmission of the parasite.

## 4 | MATERIALS AND METHODS

### 4.1 | Phylogenetic analysis of putative phospholipase candidates

For the six *P. falciparum* target proteins (Table S1), we performed a BLAST search (blastp) in the Refseq protein database limited to the representative taxa concerned (Table S1). The following information was recorded for the top hit: coverage (percentage of the query sequence covered by the NCBI hit), identity (percentage of identical amino acids between the query and hit), e-value

(the number of hits expected to be seen by chance). To confirm the ortholog relationships, we then performed reciprocal BLAST searches by (i) taking the top hits of each species and (ii) querying them against the *P. falciparum* protein database. Plots were generated using R (version 4.3.1 (R Core Team, 2023)) and its libraries (ggplot2, tibble and tidyverse) (Müller & Wickham, 2023; Wickham, 2016; Wickham et al., 2019).

### 4.2 | Cloning of SLI-based targeting constructs

For the generation of SLI-based tagging constructs, we exchanged the GFP coding sequence of pSLI-GFP (Birnbaum et al., 2017) by mScarlet. For this, we first generated the intermediate construct pSLI-PF3D7\_0924000-GFP by amplifying the C-terminal 973 bp of the coding sequence by PCR using primers PF3D7\_0924000-TAG-fw/PF3D7\_0924000-TAG-rev, starting with a stop codon, to serve as homology region for single-crossover based integration, followed by cloning the PCR product using NotI/MluI into pSLI-GFP. Subsequently, we amplified the mScarlet coding sequence from SP-mScarlet (Mesén-Ramírez et al., 2019) using primers mScarlet-fw/mScarlet-rev and cloned it via AvrII/Sall into pSLI-PF3D7\_0924000-GFP, thereby replacing the GFP cassette. This resulted in the final targeting plasmid pSLI-PF3D7\_0924000-mScarlet. For generation of the other mScarlet-tagging constructs, the respective C-terminal targeting sequences were amplified by PCR, starting with a stop codon, and cloned using NotI/MluI into pSLI-PF3D7\_0924000-mScarlet.

For generation of the pSLI-PF3D7\_1476700-mNeonGreen-glmS construct, the 963 bp C-terminal region of *pf3d7\_1476700* was amplified by PCR using primers PF3D7\_1476700-TAG-fw/PF3D7\_1476700-TAG-rev and cloned into pSLI-mNeonGreen-glmS (kindly provided by Arne Alder) using NotI/MluI. The pSLI-mNeonGreen-glmS vector is based on pSLI-GFP-glmS (Burda et al., 2020) but contains the mNeonGreen coding sequence (Shaner et al., 2013) instead of the one of GFP.

For the generation of the SLI-based TGD construct pSLI-PF3D7\_1476700-TGD, 423 bp immediately downstream of the start ATG of the *lpl1* gene were amplified by PCR using primers PF3D7\_1476700-KO-fw/PF3D7\_1476700-KO-rev and cloned using NotI/MluI into pSLI-GFP (Birnbaum et al., 2017) to generate the final targeting plasmid. The generation of all other employed pSLI-based TGD constructs was described previously (Burda et al., 2023).

Phusion High-Fidelity DNA polymerase (New England BioLabs) was used for all plasmid constructions and all plasmid sequences were confirmed by Sanger sequencing. For sequences of oligonucleotides used in this study see Table S2.

### 4.3 | *P. falciparum* culture

Blood stages of 3D7 and NF54 *P. falciparum* parasites and transgenic derivatives were cultured in human RBCs. Cultures were

maintained at 37°C in an atmosphere of 94% nitrogen, 5% carbon dioxide, and 1% oxygen using RPMI complete medium containing 0.5% Albumax according to standard procedures (Trager & Jensen, 1976). If not stated otherwise, medium was supplemented with 2 mM choline. Cultures of NF54/iGP2-based parasites were cultured in the presence of 2.5 mM glucosamine (GlcN) to prevent overexpression of the gametocyte commitment factor GDV1 (Boltryk et al., 2021).

#### 4.4 | Generation of SLI-based parasite lines

For transfection of constructs, Percoll (GE Healthcare)-enriched synchronized mature schizonts were electroporated with 50 µg of plasmid DNA using a Lonza Nucleofector II device (Moon et al., 2013). Transfectants were selected in medium supplemented with 3 nM WR99210 (Jacobus Pharmaceuticals). For generation of stable integrant cell lines, parasites containing the episomal plasmids selected with WR99210 were grown with 400 µg/mL Neomycin/G418 (Sigma) to select for transgenic parasites carrying the desired genomic modification as described previously (Birnbaum et al., 2017). Successful integration was confirmed by diagnostic PCR using FIREpol DNA polymerase (Solis BioDyne). For primer sequences see Table S2.

#### 4.5 | Production of synchronous *P. falciparum* gametocytes

Gametocytes of NF54/iGP2-derived parasites were induced as previously described (Boltryk et al., 2021). For this, synchronous ring stage cultures (2%–3% parasitemia) were washed in medium to remove remaining GlcN and plated at 2.5%–5% hematocrit in culture medium without GlcN (= day -1 of gametocyte development). After reinvasion of committed rings (= day 1 of gametocyte development), asexual parasites were depleted using 50 mM N-acetyl-D-glucosamine (GlcNAc) in the culture medium. GlcNAc was added to the cell culture medium until day 6. From day 7 until day 14, gametocyte cultures were fed with culture medium containing 0.25% Albumax +5% human serum. Gametocytes were cultured in the presence of GlcN from day 1 onwards and gametocyte cultures were fed daily.

Induction of 3D7-derived gametocytes was performed as previously described (Filarsky et al., 2018). To this aim, synchronous ring stage cultures were washed twice and then cultivated in medium without choline (= day -1 of gametocyte development). From day 1 of gametocyte development until day 6, asexual parasites were depleted using 50 mM GlcNAc in the culture medium (now again containing choline). From day 7 until day 14, gametocyte cultures were fed with culture medium containing 0.25% Albumax +5% human serum and choline. Gametocyte cultures were fed daily. Gametocyte stages and gametocytemia were monitored using Giemsa-stained thin blood smears.

#### 4.6 | Western blot analysis

Schizonts or gametocytes were purified with Percoll and resuspended in SDS sample buffer followed by heating the samples at 95°C for 5 min. Samples were resolved by SDS-PAGE and transferred to nitrocellulose membranes (LICOR). Membranes were blocked in 5% milk in TBS followed by incubation in the following primary antibodies that were diluted in TBS-Tween (0.02% Tween 20): mouse anti-RFP (ChromoTek, clone 6G6, diluted 1:2000), mouse anti-mNeonGreen (ChromoTek, clone 32F6, diluted 1:2000). After 3× washing in TBS-Tween, membranes were incubated in 5% milk in TBS-Tween containing the following secondary antibody: goat anti-mouse-800 CW (LICOR, diluted 1:10,000). Subsequently, membranes were washed another three times with TBS-Tween and scanned on a LICOR Odyssey FC imager.

#### 4.7 | Live-cell microscopy

For staining of nuclei, parasites were incubated with 0.45 µg/mL Hoechst in culture medium for 30 min at 37°C. Images were acquired on a Leica D6B fluorescence microscope, equipped with a Leica DFC9000 GT camera and a Leica Plan Apochromat 100×/1.4 oil objective. Image processing was performed using ImageJ and representative images were adjusted for brightness and contrast.

#### 4.8 | Immunofluorescence assay

Schizonts were smeared onto glass slides and air dried. A circle was drawn around the staining areas with a DAKO pen for fixation and antibody application. Schizonts were fixed with 4% paraformaldehyde in PBS for 30 min, permeabilized with 0.1% Triton X-100 in PBS for 10 min and blocked in 3% BSA in PBS for 1 h. Slides were incubated for 1 h with combinations of the following primary antibodies in 3% BSA in PBS with 0.5% Tween 20: mouse anti-RAP1 (Hall et al., 1983) (diluted 1:1000), rat anti-AMA1 4G2 (Kocken et al., 1998) (diluted 1:1000) and chicken-anti-RFP (Synaptic Systems, Cat. No. 409006, diluted 1:200). After washing, schizonts were incubated for 1 h with combinations of the following secondary antibodies in 3% BSA in PBS with 0.5% Tween 20 additionally containing 1 µg/mL DAPI: goat anti-mouse-AlexaFluor488 (Invitrogen, diluted 1:1000), goat anti-rat-AlexaFluor488 (Invitrogen, diluted 1:1000), goat anti-chicken-AlexaFluor594 (Invitrogen, diluted 1:1000). After washing, slides were mounted using DAKO mounting solution and imaged using a Zeiss LSM880 confocal microscope with a Plan-Apochromat 63×/1.40 Oil DIC M27 objective lens using the 405, 488, and 594 nm lasers. Single-plane snapshots were taken and images were processed using Airyscan processing and ImageJ.

## 4.9 | Growth analysis of mutant parasites

For asexual blood stage growth analysis of parasites, schizont stage parasites were isolated by Percoll enrichment and incubated with uninfected RBCs (5% hematocrit) for 3 h to allow rupture and invasion. Parasites were then treated with 5% sorbitol to remove residual unruptured schizonts, leading to a synchronous ring stage culture with a 3-h window. These were allowed to mature to trophozoites for 1 day and parasitemia was determined by flow cytometry and adjusted to exactly 0.1% starting parasitemia in a 2 mL dish. Medium was changed daily and growth of the parasite lines was assessed by flow cytometry over three intraerythrocytic cycles when parasites were in the trophozoite stage. As a reference, WT parasites were included in each assay.

## 4.10 | Flow cytometry

Flow cytometry-based analysis of parasite lines was performed essentially as described previously (Malleret et al., 2011). In brief, 20  $\mu$ L resuspended parasite culture were incubated with dihydroethidium (5  $\mu$ g/mL, Cayman) and SYBR Green I dye (0.25  $\times$  dilution, Invitrogen) in a final volume of 100  $\mu$ L medium for 20 min at room temperature protected from light. Samples were analyzed on a ACEA NovoCyte flow cytometer. RBCs were gated based on their forward and side scatter parameters. For every sample, 100,000 events were recorded and parasitemia was determined based on SYBR Green I fluorescence.

## 4.11 | Imaging-based gametocyte egress assay

On day 14 of gametocyte development, the egress of mature male and female gametocytes was tested as described previously (Suarez-Cortés et al., 2014) with minor modifications. In brief, parasite-infected RBC were stained with iFluor555-WGA (Biomol, stock 2 mg/mL, final concentration 5  $\mu$ g/mL) and 0.45  $\mu$ g/mL Hoechst at 37°C. After 30 min, the samples were washed in prewarmed Ringer solution and 5  $\mu$ L were placed on a slide and immediately covered with a cover slip. Imaging of this non-activated control was performed for 20 min. To study egress, gametocytes were activated by incubation in ookinete medium for 20 min at 26°C before imaging for 20 min at room temperature. Ookinete medium was prepared by supplementing culture medium (without serum or albumax) with 100  $\mu$ M Xanthurenic acid and adjusting the pH to 8.0, followed by addition of 20% human serum.

## 4.12 | Gametocyte exflagellation assay

From day 11 until day 14 of gametocytogenesis, exflagellation was determined daily in technical duplicates. 250  $\mu$ L of resuspended gametocyte culture were spun down in an Eppendorf tube at 800  $\times$  g

for 1 min. The supernatant was discarded and the pellet was resuspended in 250  $\mu$ L prewarmed (26°C) ookinete medium. Gametocytes were incubated for 12 min at 26°C. Then, 6  $\mu$ L were placed on a slide and covered with a coverslip. For 5 min, all gametocytes as well as exflagellation events were counted using a 40 $\times$  oil objective (aperture closed as much as possible to contrast the hemozoin). If indicated, the observation time was extended for another 10 min to detect a potential delay in exflagellation in non-exflagellating mutants.

## 4.13 | Statistical analysis

For statistical analysis of differences between two groups, unpaired two-tailed students t-tests were used. All statistical tests were done in GraphPad Prism. *p* values of <0.05 were considered significant. Statistical details (n numbers, test used, definition of the error bars) are described in the figure legends.

## AUTHOR CONTRIBUTIONS

**Paul-Christian Burda:** Conceptualization; data curation; formal analysis; funding acquisition; investigation; project administration; supervision; validation; visualization; writing – original draft; writing – review and editing; methodology. **Emma Pietsch:** Conceptualization; investigation; writing – review and editing; visualization; validation; methodology; formal analysis; data curation. **Korbinian Niedermüller:** Investigation; formal analysis; validation. **Mia Andrews:** Investigation; validation; formal analysis. **Britta S. Meyer:** Visualization; investigation; validation; formal analysis. **Tobias L. Lenz:** Investigation; validation; visualization; formal analysis. **Danny W. Wilson:** Formal analysis; validation. **Tim-Wolf Gilberger:** Funding acquisition; writing – review and editing; formal analysis; validation.

## ACKNOWLEDGMENTS

We thank Arne Alder for providing the pSLI-mNeonGreen-glmS vector. We acknowledge the Advanced Light and Fluorescence Microscopy (ALFM) facility at the Centre for Structural Systems Biology (CSSB) for support with image recording and analysis. This work was supported by a grant from the German Research Foundation (Deutsche Forschungsgemeinschaft, DFG) to PCB (project number 414222880). KN was funded by a grant from the DFG within the SPP2225 to TWG and PCB (project number 446556156). DWW was funded by an Alexander Von Humboldt Fellowship, MA by an Australian Research Council RTP scholarship and DWW, TWG, MA by a DAAD/Universities Australia Collaborative Research Grant. Open Access funding enabled and organized by Projekt DEAL.

## CONFLICT OF INTEREST STATEMENT

The authors declare that they have no conflict of interest.

## DATA AVAILABILITY STATEMENT

All data generated or analyzed during this study are included in this published article and its supplemental material files.

## ETHICS STATEMENT

Erythrocyte concentrates were purchased from the University Medical Center Hamburg-Eppendorf (approval number 10569a/96-1). Erythrocyte concentrates are anonymous and age or gender of the blood donors were not known. Antibodies used in this study were purchased commercially.

## ORCID

Emma Pietsch  <https://orcid.org/0000-0003-4744-1666>

Mia Andrews  <https://orcid.org/0000-0002-3547-8130>

Britta S. Meyer  <https://orcid.org/0000-0002-2549-1825>

Tobias L. Lenz  <https://orcid.org/0000-0002-7203-0044>

Danny W. Wilson  <https://orcid.org/0000-0002-5073-1405>

Tim-Wolf Gilberger  <https://orcid.org/0000-0002-7965-8272>

Paul-Christian Burda  <https://orcid.org/0000-0003-0461-4352>

## REFERENCES

- Asad, M., Yamaryo-Botté, Y., Hossain, M.E., Thakur, V., Jain, S., Datta, G. et al. (2021) An essential vesicular-trafficking phospholipase mediates neutral lipid synthesis and contributes to hemozoin formation in *Plasmodium falciparum*. *BMC Biology*, 19, 159.
- Aurrecochea, C., Brestelli, J., Brunk, B.P., Dommer, J., Fischer, S., Gajria, B. et al. (2009) PlasmoDB: a functional genomic database for malaria parasites. *Nucleic Acids Research*, 37, D539–D543.
- Bennink, S., Kiesow, M.J. & Pradel, G. (2016) The development of malaria parasites in the mosquito midgut. *Cellular Microbiology*, 18, 905–918.
- Birnbaum, J., Flemming, S., Reichard, N., Soares, A.B., Mesén-Ramírez, P., Jonscher, E. et al. (2017) A genetic system to study *Plasmodium falciparum* protein function. *Nature Methods*, 14, 450–456.
- Boltryk, S.D., Passecker, A., Alder, A., Carrington, E., van de Vegte-Bolmer, M., van Gemert, G.-J. et al. (2021) CRISPR/Cas9-engineered inducible gametocyte producer lines as a valuable tool for *Plasmodium falciparum* malaria transmission research. *Nature Communications*, 12, 4806.
- Burda, P.-C., Crosskey, T., Lauk, K., Zurborg, A., Söhnchen, C., Liffner, B. et al. (2020) Structure-based identification and functional characterization of a Lipocalin in the malaria parasite *Plasmodium falciparum*. *Cell Reports*, 31, 107817.
- Burda, P.-C., Ramaprasad, A., Bielfeld, S., Pietsch, E., Weitalla, A., Söhnchen, C. et al. (2023) Global analysis of putative phospholipases in *Plasmodium falciparum* reveals an essential role of the phosphoinositide-specific phospholipase C in parasite maturation. *mBio*, 14, e0141323.
- Burda, P.C., Roelli, M.A., Schaffner, M., Khan, S.M., Janse, C.J. & Heussler, V.T. (2015) A plasmodium phospholipase is involved in disruption of the liver stage parasitophorous vacuole membrane. *PLoS Pathogens*, 11, e1004760.
- Burda, P.-C., Schaffner, M., Kaiser, G., Roques, M., Zuber, B. & Heussler, V.T. (2017) A plasmodium plasma membrane reporter reveals membrane dynamics by live-cell microscopy. *Scientific Reports*, 7, 9740.
- Coleman, J.E. (1992) Structure and mechanism of alkaline phosphatase. *Annual Review of Biophysics and Biomolecular Structure*, 21, 441–483.
- Deligianni, E., Morgan, R.N., Bertuccini, L., Wirth, C.C., Silmon de Monerri, N.C., Spanos, L. et al. (2013) A perforin-like protein mediates disruption of the erythrocyte membrane during egress of *Plasmodium berghei* male gametocytes. *Cellular Microbiology*, 15, 1438–1455.
- Desai, N.A. & Shankar, V. (2003) Single-strand-specific nucleases. *FEMS Microbiology Reviews*, 26, 457–491.
- Filarsky, M., Fraschka, S.A., Niederwieser, I., Brancucci, N.M.B., Carrington, E., Carrió, E. et al. (2018) GDV1 induces sexual commitment of malaria parasites by antagonizing HP1-dependent gene silencing. *Science* (1979), 359, 1259–1263.
- Flammersfeld, A., Panyot, A., Yamaryo-Botté, Y., Aurass, P., Przyborski, J.M., Flieger, A. et al. (2020) A patatin-like phospholipase functions during gametocyte induction in the malaria parasite *Plasmodium falciparum*. *Cellular Microbiology*, 22, e13146.
- Flieger, A., Frischknecht, F., Häcker, G., Horne, M.W. & Pradel, G. (2018) Pathways of host cell exit by intracellular pathogens. *Microbial Cell*, 5, 525–544.
- Florens, L., Washburn, M.P., Raine, J.D., Anthony, R.M., Grainger, M., Haynes, J.D. et al. (2002) A proteomic view of the *Plasmodium falciparum* life cycle. *Nature*, 419, 520–526.
- Hall, R., McBride, J., Morgan, G., Tait, A., Werner Zolg, J., Walliker, D. et al. (1983) Antigens of the erythrocytic stages of the human malaria parasite *Plasmodium falciparum* detected by monoclonal antibodies. *Molecular and Biochemical Parasitology*, 7, 247–265.
- Istvan, E.S., Mallari, J.P., Corey, V.C., Dharia, N.V., Marshall, G.R., Winzeler, E.A. et al. (2017) Esterase mutation is a mechanism of resistance to antimalarial compounds. *Nature Communications*, 8, 14240.
- Kocken, C.H.M., Van Der Wel, A.M., Dubbeld, M.A., Narum, D.L., Van De Rijke, F.M., Van Gemert, G.J. et al. (1998) Precise timing of expression of a *Plasmodium falciparum*-derived transgene in *Plasmodium berghei* is a critical determinant of subsequent subcellular localization. *The Journal of Biological Chemistry*, 273, 15119–15124.
- Kuehn, A. & Pradel, G. (2010) The coming-out of malaria gametocytes. *Journal of Biomedicine & Biotechnology*, 2010, 11.
- Lasonder, E., Rijpmma, S.R., Van Schaijk, B.C.L., Hoeijmakers, W.A.M., Kensche, P.R., Gresnigt, M.S. et al. (2016) Integrated transcriptomic and proteomic analyses of *P. falciparum* gametocytes: molecular insight into sex-specific processes and translational repression. *Nucleic Acids Research*, 44, 6087–6101.
- López-Barragán, M.J., Lemieux, J., Quiñones, M., Williamson, K.C., Molina-Cruz, A., Cui, K. et al. (2011) Directional gene expression and antisense transcripts in sexual and asexual stages of *Plasmodium falciparum*. *BMC Genomics*, 12, 587.
- Malleret, B., Claser, C., Ong, A.S.M., Suwanarusk, R., Sriprawat, K., Howland, S.W. et al. (2011) A rapid and robust tri-color flow cytometry assay for monitoring malaria parasite development. *Scientific Reports*, 1, 118.
- Mesén-Ramírez, P., Bergmann, B., Tran, T.T., Garten, M., Stäcker, J., Naranjo-Prado, I. et al. (2019) EXP1 is critical for nutrient uptake across the parasitophorous vacuole membrane of malaria parasites. *PLoS Biology*, 17, e3000473.
- Moon, R.W., Hall, J., Rangkuti, F., Ho, Y.S., Almond, N., Mitchell, G.H. et al. (2013) Adaptation of the genetically tractable malaria pathogen *Plasmodium knowlesi* to continuous culture in human erythrocytes. *Proceedings of the National Academy of Sciences of the United States of America*, 110, 531–536.
- Müller, K. & Wickham, H. (2023) tibble: simple data frames. <https://tibble.tidyverse.org/>
- Pietsch, E., Ramaprasad, A., Bielfeld, S., Wohlfarter, Y., Maco, B., Niedermüller, K. et al. (2023) A patatin-like phospholipase is important for mitochondrial function in malaria parasites. *mBio*, e0171823.
- R Core Team. (2023) R: a language and environment for statistical computing. <https://www.R-project.org>
- Ramaprasad, A., Burda, P.C., Koussis, K., Thomas, J.A., Pietsch, E., Calvani, E. et al. (2023) A malaria parasite phospholipase facilitates efficient asexual blood stage egress. *PLoS Pathogens*, 19, e1011449.
- Shaner, N.C., Lambert, G.G., Chammass, A., Ni, Y., Cranfill, P.J., Baird, M.A. et al. (2013) A bright monomeric green fluorescent protein derived from *Branchiostoma lanceolatum*. *Nature Methods*, 10, 407–409.



- Shunmugam, S., Quansah, N., Flammersfeld, A., Islam, M.M., Sassmannshausen, J., Bennink, S. et al. (2023) The patatin-like phospholipase PfPNPLA2 is involved in the mitochondrial degradation of phosphatidylglycerol during *Plasmodium falciparum* blood stage development. *Frontiers in Cellular and Infection Microbiology*, 13, 997245.
- Silvestrini, F., Lasonder, E., Olivieri, A., Camarda, G., van Schaijk, B., Sanchez, M. et al. (2010) Protein export marks the early phase of gametocytogenesis of the human malaria parasite *Plasmodium falciparum*. *Molecular & Cellular Proteomics*, 9, 1437–1448.
- Singh, P., Alagunan, A., More, K.R., Lorthiois, A., Thiberge, S., Gorgette, O. et al. (2019) Role of a patatin-like phospholipase in *Plasmodium falciparum* gametogenesis and malaria transmission. *Proceedings of the National Academy of Sciences of the United States of America*, 116, 17498–17508.
- Suarez-Cortés, P., Silvestrini, F. & Alano, P. (2014) A fast, non-invasive, quantitative staining protocol provides insights in *Plasmodium falciparum* gamete egress and in the role of osmiophilic bodies. *Malaria Journal*, 13, 389.
- Trager, W. & Jensen, J.B. (1976) Human malaria parasites in continuous culture. *Science* (1979), 193, 673–675.
- Wickham, H. (2016) *ggplot2*, 2nd edition. Cham: Springer International Publishing.
- Wickham, H., Averick, M., Bryan, J., Chang, W., McGowan, L., François, R. et al. (2019) Welcome to the Tidyverse. *Journal of Open Source Software*, 4, 1686.
- Wilson, S.K., Heckendorn, J., Di Genova, B.M., Koch, L.L., Rooney, P.J., Morrisette, N. et al. (2020) A toxoplasma gondii patatin-like phospholipase contributes to host cell invasion. *PLoS Pathogens*, 16, e1008650.
- Wirth, C.C., Glushakova, S., Scheuermayer, M., Repnik, U., Garg, S., Schaack, D. et al. (2014) Perforin-like protein PPLP2 permeabilizes the red blood cell membrane during egress of *Plasmodium falciparum* gametocytes. *Cellular Microbiology*, 16, 709–733.

## SUPPORTING INFORMATION

Additional supporting information can be found online in the Supporting Information section at the end of this article.

**How to cite this article:** Pietsch, E., Niedermüller, K., Andrews, M., Meyer, B.S., Lenz, T.L., Wilson, D.W. et al. (2024) Disruption of a *Plasmodium falciparum* patatin-like phospholipase delays male gametocyte exflagellation. *Molecular Microbiology*, 121, 529–542. Available from: <https://doi.org/10.1111/mmi.15211>